Materials Science-Poland, 41(2), 2023, pp. 401-413
http://www.materialsscience.pwr.wroc.pl/
DOI: 10.2478/msp-2023-0027

sciendo

Numerical and experimental analysis of the notch effect on fatigue behavior of polymethylmethacrylate metal based on strain energy density method and the extended finite element method

Mustafa Moussaoui[1]*, Abdelkhader Bendriss[1], Antar Tahiri[1], Ahmed Kellai[2], Souad Zergod[1], Hamza Djeloud[1], Brahim Kalil Hachi[1]

[1]Laboratory for Mechanics and Materials Development at ZianeAchour University in the City of Djelfa in Algeria
[2]Research Center in Industrial Technologies, CRTI, P.O. Box 64, Cheraga, 16014 Algiers, Algeria

This work investigates the effect of the notch on fatigue behavior by combining two methods: the extended finite element method (XFEM) and the averaged strain energy density (ASED) method, which considers the combined action of bending and shear loading. The ASED method has already been proven accurate for assessing the failure of components in the presence of sharp and blunt notches, and several results are available in the literature for different materials. These results were compared with those obtained from the experimental tests reported here. The main purpose of this study was twofold: The first part is an experimental study of fatigue in rotary bending of specimens weakened by U and V notches made of polymethyl-methacrylate (PMMA) material. Two values for the radius were used for the U-notches (0.2 and 2 mm) and two angles for the V-notches (20° and 140°). The second part of the study consisted of performing several simulation tests using the Cast3m software for different angles and radii. The local approach based on the mean value of the ASED acted over a finite-sized volume surrounding the highly stressed regions. The maximum principal stress located at the notch edge defined the center of the control volume. If the notch is blunt, the control volume assumes a crescent shape with its width measured along the notch bisector line. When the notch is considered pointed (V-notched) or is a crack, the control volume becomes a circle with its center at the notch tip. The presence of geometric discontinuities in structures affects their lifetime by reducing it, producing a high concentration of local energy around the notch tip. Good convergence was obtained between the numerical simulation and experimental results for the ASED in a finished zone surrounding the notch tip.

Keywords: *fatigue failure, notch, averaged strain energy density, mixed mode I/II, CV - control volume*

1. Introduction

Fatigue failure is a common state of failure in mechanical components that operate under cyclic loading. It is particularly rapid in materials that exhibit brittle behavior, especially for components subjected to bending. Fatigue failure is also more likely to occur in components with geometric discontinuities or defects, such as those resulting from manufacturing or from the migration of inclusions during the elaboration of the materials. These geometric changes can be created intentionally (e.g., holes, grooves, shoulders) or accidentally during service. Shapes that we can consider as geometric discontinuities are notches, whether in blunt-U shape or acute V shape. These shapes are the subject of several studies by researchers in the field of fracture [1–3] and fatigue fracture [4–7] of samples. The presence of these notches in mechanical organs generally induces amplifications of the stresses and becomes a privileged place of stress concentration; several authors are interested in the effects of their presence in mechanical components. A.R. Torabi et al. [1] studied the brittle fracture of Brazilian disks containing central V-notches with end holes (VO-notches) made of polymethylmethacrylate (PMMA) under mode II loading. They used the averaged strain energy

* E-mails: m.moussaoui@univ-djelfa.dz; moussaoui_must@yahoo.fr

© Mustafa Moussaoui et al. 2023. This is an open access article distributed under the Creative Commons Attribution-NonCommercial-NoDerivatives 4.0 License. (http://creativecommons.org/licenses/by-nc-nd/4.0/)

density (ASED) criterion, and their contributions demonstrated that the ASED approach works well on specimens containing VO-notches in pure mode II. This approach was used by Lazzarin and Zambardi [8] to predict the static and fatigue behavior of components weakened by sharp re-entrant corners, showing that strain energy density (SED) can accurately predict the static and fatigue behavior of heavily notched components. Berto and Lazzarin [9] applied the SED approach to static and fatigue strength assessments of notched and welded structures. These authors indicated that the region around the tip of the notch is controlled by a finite size volume and when sharp V-shaped cracks or notches are considered, the volume becomes a circle or a circular sector, where the radius R0 is the measured size of this circular sector. This parameter R0 has become a propriety of a material, and it depends on a fracture toughness, ultimate tensile strength, and Poisson's ratio in the case of static loads; it depends on the fatigue strength of the butt ground welded joints and the notch stress intensity factor (NSIF) range in the case of welded joints under high cycle fatigue loading. On the basis of the local energy concept, Aliha et al. [10] used it in their article analyzing cracked specimens (semicircular and triangular crack type) of four different shapes made by PMMA material under pure mode I, pure mode II, and mixed mode I/II. They demonstrated through experimental work that the SED approach can be used as a criterion to predict the behavior of crack specimens under mixed-mode loading.

According to M. Aliha et al. [11], the ASED criterion has been used for evaluating brittle fracture behavior for edge-cracked triangular specimens subjected to symmetric, three-point bend loading, caused by rock materials. It was found that the ASED criterion can successfully predict the fracture loads of investigated marble in the entire range of mode I/II mixities.

Negru et al. [12] used the local SED approach with a theory of critical distance (TCD) for evaluation of brittle fracture of two types of specimens: single edge notched bend (SENB) U-notched specimens and asymmetric semi-circular bend (ASCB) cracked specimens. The specimens were submited to bend loading to predict maximum fracture load for two different polyurethane (PUR) materials. Both criteria have proven their effectiveness in predicting the fracture load. Ayatollahi, Berto, and Lazzarin [13] examined a mixed mode of Brazilian disk samples containing sharp and blunt V-notches made of polycrystalline graphite. The ASEFD is used over a well-defined volume to predict static strength for different values of loading mixtures, V-notch angles, and notch radii [14]. Many researches have focused their studies on mixed mode loading based on the use of the SED criterion to predict the failure of a notched specimen [10]. Salavati et al. [15] and Torabi and Berto [3] employed bainitic functionally graded steels and a generalized ASED criterion to investigate the fracture behavior of brittle and quasi-brittle materials, respectively, for two cracked specimens: a cracked Brazilian disk (BD) specimen and a semicircular bend (SCB) specimen under mixed mode I/II loading. The stress intensity factors K_I and K_{II} were combined with T-stress computed from ASED in a control volume around the crack tip. Two criteria were used by Li, Fantuzzi, and Tornabene [16]: SED and maximum tangential stress criteria to evaluate the initial crack growth angles and the dimensionless stress-intensity factors.

This collected research, which was oriented towards the use of the SED approach, has proven that this approach has high reliability in the prediction and evaluation of the parameters governing the behavior of fracture and the fatigue fracture.

On the basis of this research, the objective of this paper is to investigate the effect of notches on fatigue behavior by combining two methods, the extended finite element method (XFEM) and the ASED approach under mixed-mode loading I/II. Experimental tests are conducted on cylindrical specimens notched with two types of notches: blunt U-notches and sharp V-notches made by polymethylmethacrylate (PMMA) material. The obtained results are compared with those obtained experimentally and show good agreement with the numerical results.

2. Materials and methods

The material considered in this study is PMMA, polymethyl methacrylate. It exhibits fragile behavior. PMMA has the following properties:

Experimental rotary bending fatigue tests are performed on the SM1090 machine (see Fig. 1). The recommended specimens are cylindrical in shape (Fig. 2). The specimens are mounted on the rotary bending fatigue machine with one end fixed on the chuck while the other end is subjected to a constant force at a frequency of 50 Hz.

Given the difficulty of machining notches on this type of material, we were able to adopt two different notches for the two configurations of U and V notches. For the sharp V notches, we chose two angles with dimensions of 20° and 140° and for the blunt U notches, we chose two radii of 0.2 mm and 2 mm (see Figs. 2 and 3). The recommended specimen geometries suitable for the rotary bending fatigue machine are cylindrical shapes with the dimensions shown in Figure 3.

3. Theoretical concept of strain energy density approach

The assessment of the risk of failure for a structure subjected to fatigue is based on failure criteria that designers consider in their designs. To predict the fatigue behavior of the mixed mode surrounding the tip notch, an energy criterion was formalized by Sih [17], which gave a theoretical basis to Gillemot's experiment [17, 18]. The energy criterion was strongly supported by several researchers, and it offered an alternative approach that could be used to characterize the level of stress at the tip notch without recourse to mesh fineness around the tip notch. He postulated that the failure occurs when the quantity of energy reaches a critical value of S_c, while the direction of crack propagation was determined by imposing a minimum condition on S [17, 19, 20].

The basic idea of the strain energy density criterion consisted of considering a finite size volume around the notch over which the strain energy is averaged [8, 21]. According to this criterion, fracture occurs when the variation of local energy over the structural volume $\triangle W$ reaches a critical value, W_c, that characterizes the material parameter [22].

$$\triangle W = W_c \tag{1}$$

When two modes act together in the case of mixed mode I/II loading, the total critical strain energy density can be evaluated according to the following equation, which is valid for both unnotched and notched components [10]. The expression can be written as follows:

$$W_c = \frac{\sigma_t^2}{2E} + \frac{\tau_t^2}{2E} \tag{2}$$

where σ_t is the ultimate tensile stress of a flat specimen and τ_t is the ultimate shear strength of the unnotched material. These can be calculated approximately as:

$$\tau_t = \sigma_t / 2\sqrt{2(1+\nu)} \tag{3}$$

with ν is Poisson's coefficient.

3.1. Stress distribution at V notch

Using the Williams' series expansions [23, 24], the stress relationships can be expressed nearness of the notch tip as follow:

$$\begin{Bmatrix} \sigma_{\theta\theta} \\ \sigma_{rr} \\ \tau_{r\theta} \end{Bmatrix} = \sum_{i=1}^{2} \lambda_i \, r^{\lambda_i - 1} a_i \begin{Bmatrix} f_{i,\theta}(\theta) \\ f_{i,r}(\theta) \\ f_{i,r\theta}(\theta) \end{Bmatrix} \tag{4}$$

Table 1. Mechanical properties of PMMA

Tensile strength (MPa)	**Flexural strength (MPa)**	**Modulus of elasticity (MPa)**	**Density (kg/m^3)**	**Elongation (%)**	**Poisson's rate**	**Fracture Toughness (MPa.$\sqrt{}$m)**
70.5	110	3000	1190	6	0.3	1.863

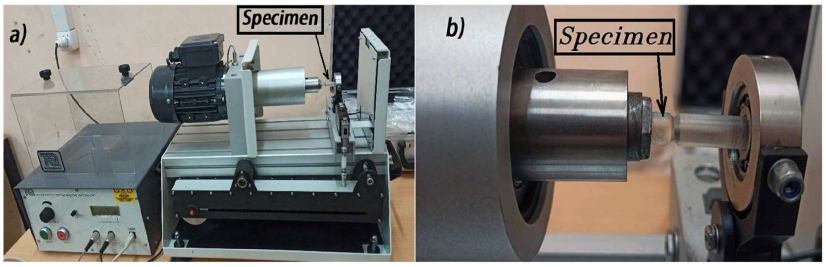


Fig. 1. Rotary bending fatigue machine SM1090

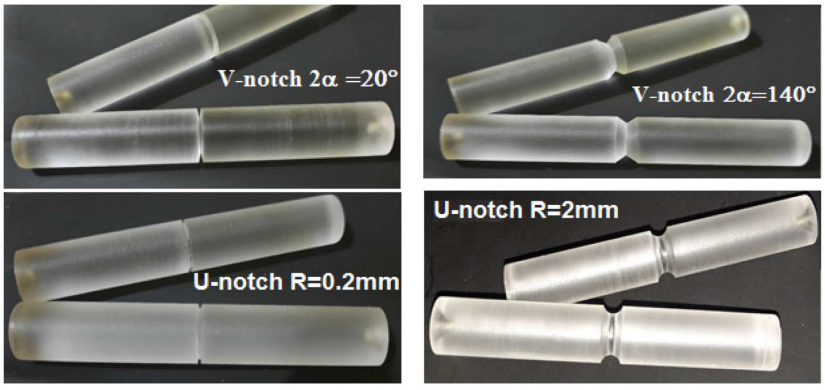


Fig. 2. Manufacture of notched specimens

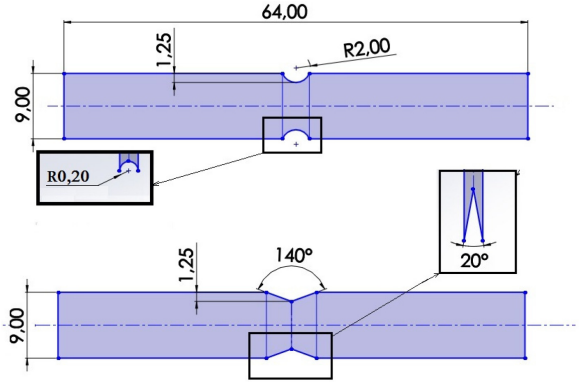


Fig. 3. Recommended specimen sizes

where $\lambda_i (i = 1, 2)$ are characteristic values that are dependent on the notch opening angle (Fig. 1) [8]; r is the distance from notch tip; and a_i (i = 1, 2) are defined as [24–26]:

$$a_1 = \frac{K_1^N}{\lambda_1 \sqrt{2\pi}\left[(1+\lambda_1)+\chi_1(1-\lambda_1)\right]},$$

$$a_2 = \frac{K_2^N}{\lambda_2 \sqrt{2\pi}\left[(1+\lambda_2)+\chi_2(1-\lambda_2)\right]}$$

And $f_1(\theta)$, $f_2(\theta)$ represents stress functions that correspond to symmetric (Mode I) and ant-symmetric (Mode II) components, respectively, and their expressions are given in [8, 24, 25], K_1^N, K_2^N are the notch stress intensity factors (NSIFs) that correspond to the opening (Mode I, i = 1) and sliding (Mode II, i = 2) modes, respectively [25]:

$$K_1^N = \sqrt{2\pi} \lim_{r \to 0} r^{1-\lambda_1} \sigma_{\theta\theta}(\theta \to 0),$$

$$K_2^N = \sqrt{2\pi} \lim_{r \to 0} r^{1-\lambda_2} \tau_{r\theta}(\theta \to 0)$$

The expression of the strain energy density in bi-dimensional problems (W) can be written at any point as [8]:

$$W = \frac{1}{2E}\Big[\sigma_{\theta\theta}^2 + \sigma_{rr}^2 + \sigma_{zz}^2 - 2\nu\left(\sigma_{\theta\theta}\sigma_{rr} + \sigma_{\theta\theta}\sigma_{zz} + \sigma_{rr}\sigma_{zz}\right) + 2(1+\nu)\,\tau_{r\theta}^2\Big] \quad (5)$$

where E is Young's modulus, and the values of stress σ_{zz} equals zero for plane stress condition and $\sigma_{zz} = \nu(\sigma_{\theta\theta} + \sigma_{rr})$ for plane strain condition.

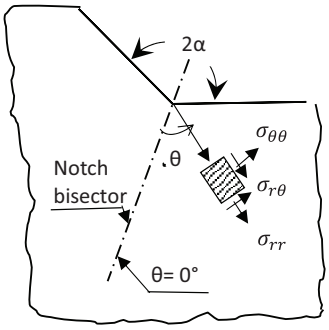


Fig. 4. Stress components located at the point of the tip of the V-notch, in a polar coordinate system

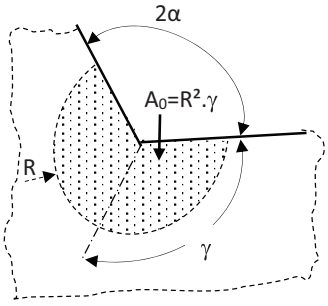


Fig. 5. Circular zone nears tip of V-notch [8], $2\gamma = 2\pi - 2\alpha$

Substituting the stress components Eq. (4) into Eq. (5), and integrating the strain energy density over a control area on a boundary defined by a distance of the radius R_0, the averaged SED ($\overline{W}$) expression can be calculated:

$$\overline{W} = \frac{1}{A_0}\int_0^{R_0}\int_{-\gamma}^{+\gamma} W.rdrd\theta \tag{6}$$

with A_0 as a zone of the control area;

The elastic strain energy density per cycle, W_e, can be formulated in terms of the stress amplitude applied and elastic modulus, E [27–29]:

$$\triangle W_e = \frac{(\triangle\sigma)^2}{2E} \tag{7}$$

In Mi et al. [30] the total strain energy density was determined by its relationship with fatigue life using the following equation without taking a plasticization [31]:

$$\triangle W_T = A(2N_f)^B \tag{8}$$

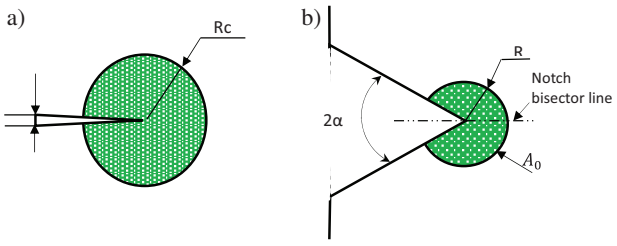


Fig. 6. Control volume A_0 for (a) sharp crack, (b) V-notch

where $(2N_f)$ is the fatigue life; A is the strain energy density coefficient; and B is the strain energy density index.

3.2. Strain energy for V-notch under mixed mode loading

For fatigue problems [9–11], the combined mode I and II can easily be evaluated by means of the SED averaged over a control volume, considered as a material property and assumed to be a circular sector of radius R_c, as shown in Figure 5, according to Lazzarin and Zambardi [8]. It becomes a circle with radius R_c in the case of cracks or V-notches in mode I or mode mixed I + II (Fig. 6). For static loading, the radius R_c can be evaluated according to the following expression:

$$R_c = \frac{(1+\nu)(5-8\nu)}{4\pi}\left(\frac{K_{Ic}}{\sigma_t}\right)^2 \tag{9}$$

Under fatigue limit conditions, R_c depends on smooth specimen fatigue limit $\triangle\sigma_0$ and on the threshold behavior $\triangle K_{th}$, [6, 32] the relationship becomes:

$$R_c = \frac{(1+\nu)(5-8\nu)}{4\pi}\left(\frac{\triangle K_{th}}{\triangle\sigma_0}\right)^2 \tag{10}$$

When the $\nu = 0.3$ equation (10) gives a critical radius:

$$R_c \approx 0.27\left(\frac{\triangle K_{th}}{\triangle\sigma_0}\right)^2 \tag{11}$$

El Haddad, Topper, and Smith [33] provide a parameter to link the stress intensity threshold term $\triangle K_{th}$ and fatigue limit $\triangle\sigma_0$ with critical crack length

$$l_0 = \left(\frac{\triangle K_{th}}{\triangle \sigma_0}\right)^2 . \frac{1}{\pi} <=> \; l_0 . \pi = \left(\frac{\triangle K_{th}}{\triangle \sigma_0}\right)^2$$

And the critical crack length can be obtained by the following expression:

$$K_{Ic} = \sigma_Y \sqrt{\pi l_0} => l_0 = \left(\frac{K_{Ic}}{\sigma_Y}\right)^2 . \frac{1}{\pi},$$

$$\text{from which } l_0 = 0.222 \text{ mm}$$

$$\left(\frac{\triangle K_{th}}{\triangle \sigma_0}\right)^2 = 0.697 \text{ mm} \cong 0.70 \text{ mm}$$

Hence, the radius of the control volume

$$R_c = 0.27 \left(\frac{\triangle K_{th}}{\triangle \sigma_0}\right)^2 = 0.189 \text{ mm}$$

In the case of a combined bending and shearing action on a component weakened by a V-notch and under conditions of linear elasticity, the SED averaged over the control volume, which embraces the notch tip, and can be calculated by means of the following expression [4, 27, 34]:

$$\triangle \overline{W}_1 = c_w \frac{e_1}{E} \left[\frac{\triangle K_1^N}{R_C^{1-\lambda_1}}\right]^2;$$

$$\triangle \overline{W}_2 = c_w \frac{e_2}{E} \left[\frac{\triangle K_2^N}{R_C^{1-\lambda_2}}\right]^2 \qquad (12)$$

where $\triangle K_1$ and $\triangle K_2$ represent the Mode I and Mode II NSIF ranges, and R_c is the critical radius of the control volume related to Mode I and Mode II loadings. The terms e_1 and e_2 indicate two parameters that summarize the dependence on the V-notch geometry. Lazzarin and Zambardi [8] propose the following approximate formulas for $\nu = 0.3$ under plane strain condition:

$$e_1 = -5.373 \times 10^{-6} (2\alpha)^2 + 6.151 \times 10^{-4} (2\alpha) + 0.133,$$

$$e_2 = 4.809 \times 10^{-6} (2\alpha)^2 - 2.346 \times 10^{-3} (2\alpha) + 0.34. \qquad (13)$$

The parameters λ_1 and λ_2 are the eigenvalues of the Williams' stress field solution for the N-SIF $\triangle K_1$ and $\triangle K_2$ for modes I and II, respectively, and (2α) is the opening angle. The evaluation of $\triangle K_1$ and $\triangle K_2$ is obtained numerically by the XFEM method from the following relationships:

$$\begin{cases} \triangle K_1 = K_{1max} - \mathrm{K}_{1min} \\ \triangle K_2 = K_{2max} - \mathrm{K}_{2min} \end{cases} \qquad (14)$$

The parameter c_w is the weighing parameter that takes into account the different loading ratio, and it is equal to 1.0 for R = 0 and 0.5 for R = −1.

In a highly stressed region, all stress and strain components are correlated to mode I and mode II (NSIF). The variation of total strain energy density averaged $\triangle W_T$ over a control volume surrounding the notch tip that can be evaluated from the following closed-form expression in a defined zone A_0 [2, 5, 30, 35]:

$$\triangle W_T = \triangle W_1 + \triangle W_2 \qquad (15)$$

In numerical computation, the averaged SED can be evaluated directly from the FE results, once the size of the control volume is properly defined, $\triangle \mathrm{W}_T$, by summation of the strain-energies $\mathrm{W}_{\mathrm{FEM,i}}$ calculated for each i-th finite element belonging to the control volume V [36]:

$$\triangle W_T = c_w \frac{\sum_V W_{FEM,i}}{V} \qquad (16)$$

3.3. Strain energy density for blunt notch under mixed-mode loading

In the case of blunt notches, the control volume is assumed to have crescent shape, with R_c being its maximum width as measured along the notch bisector line (Fig. 7b) as stated by Lazzarin and Berto [35]. Under mixed-mode conditions, the maximum principal stress σ_{Max} occurs on a notch edge point determined by the polar angle φ, out of the bisector line (Fig. 7b). The control volume is no longer centered with respect to the notch bisector, but rigidly rotated with respect to the notch bisector and centered on the point where the maximum principal stress reaches its maximum value (Fig. 7) [37–39]. This rotation is shown in Figure 7a where the control area is drawn for a U-shaped notch both under mode I loading (Fig. 7b) and mixed-mode loading (Fig. 7a). Thus, the procedure developed for mode I was extended to mixed I/II mode conditions.

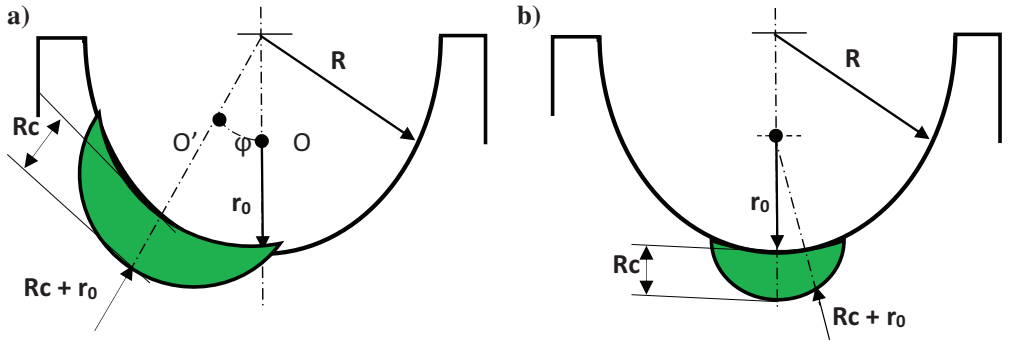


Fig. 7. Control volume for U-notch: (a) mixed-mode I/II, (b) open mode I

Dealing with blunt notches under fatigue loading, the following expression can be used to evaluate the strain energy for notches in mode I,

$$\triangle W_1 = F(2\alpha)H\left(2\alpha, \frac{R_c}{R}\right)\frac{\triangle\sigma_{tip}^2}{E} \qquad (17)$$

where F and H values are given in Berto and Lazzerin [21] as the functions of the openings angles, Poisson's ratios, and the ratio of R_c to the notch tip radius; F(2α) can be expressed by the following relationship [21]:

$$F(2\alpha) = \left(\frac{q-1}{q}\right)^{2(1-\lambda_1)}\left[\frac{\sqrt{2\pi}}{1+\tilde{w}_1}\right]^2 \qquad (18)$$

To account for the shear contribution, Lazzarin et al. [40] dealt with a torsion problem in which they developed an expression for the strain energy density over volume control for the U-notch and the blunt V-notch. from this relation we used it in the shear action that contributes to the mode –II of sliding mode, this formula is expressed as follows [22]:

$$\triangle W_2 = \omega_2\left(2\alpha, \frac{Rc}{R}\right)\frac{\triangle\tau_{max}^2}{2G} \qquad (19)$$

where, G is the shear modulus, and the value of ω_2 is taken as the same as the value reported in the torsion, and is a function of the notch opening angles and the ratio of R_c/R.

4. Numerical simulations and analysis of results

This study is divided into two parts: the first is the experimental part, realized on the rotary bending fatigue machine, which provided us with results from which we deduced curves of the average total local strain energy as a function of the number of cycles to failure (W–N$_f$). The second part is the simulation carried out by programming in the Gibiane language in the Cast3M code. The simulation takes into account different loads and different angles for the V notch and different radii for the U notch. The specimen is realized in two dimensions (Fig. 3) and having been subjected to a cyclic concentric loading at its end and embedded in the other end.

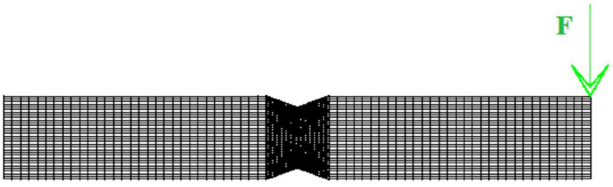


Fig. 8. Bi-dimensional finite elements model

Under the conditions of plane strain and by using the extended finite element method, the specimen is converted into discrete Q4 elements with a total number of 3224 elements (Fig. 8).

4.1. XFEM-based crack simulation

The presence of a geometric discontinuity defined by a notch in the specimen undergoing fatigue loading leads to crack initiation after a certain number of loading cycles, followed by its propagation. Numerically, the XFEM is used to represent the discontinuities independent of the mesh. The discontinuities can be modeled by enriching

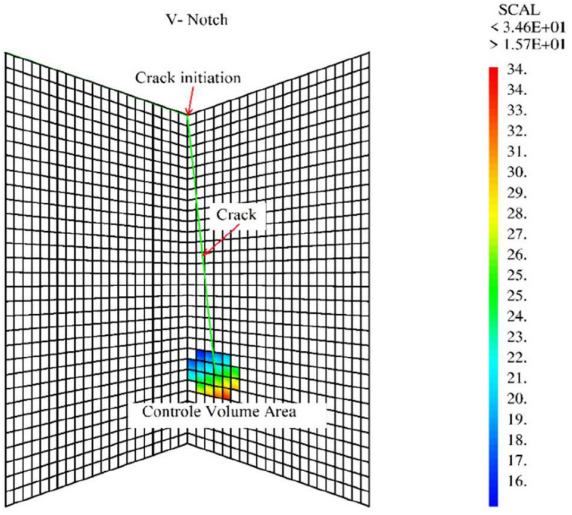


Fig. 9. Crack propagation emanating from the V notch and the location of the control volume

all discontinuous elements using enrichment functions that satisfy the discontinuous behavior and adding additional nodal degrees of freedom. It enables us to control the initiation and propagation of fatigue cracks without the need to remesh the structure.

Crack initiation is localized at the point where the principal stress criterion σ_I reaches its maximum value (see Fig. 12), triggering a zone surrounding the crack tip defined by the control volume, which follows the cracked tip during crack propagation (Fig. 9).

4.2. Effect of U and V notch on the energy distribution of notched specimens

Based on the local approach of strain energy density which consists in the first step of defining the volume control zone where it rules the elaboration of the zone damage and then leads to the initiation and propagation of cracks. This zone is located around the notch tip and includes a quantity of elastic deformation energy. If this energy reaches the value of the critical energy defined by W_c, the structure undergoes a crack initiation and rupture. A calculation is made of the total local energy, which takes into account two quantities of energy linking to the bending and shearing energies $\triangle W_T = \triangle W_1 + \triangle W_2$ normalized by the critical energy W_c described by the equations above.

Figure 10 shows the distribution of the ASED normalized by the critical energy in dimensionless units as a function of the fatigue life for the two types of notches, V and U. The results obtained are compared with those from the experiment. At low fatigue cycles, the energy values reach maximum values for both types of notches. The trend follows a decay towards a stabilization of the energy at a high life cycle. In terms of amplitude, the local energy of the sharp notch is higher than the energy values of the blunt notch, and this is due to the attenuation of the stress concentrations at the notch level. The presence of notches in a structure always leads to the amplification of energy concentrations and the reduction of the structure's lifetime. The introduction of the fatigue behavior curve of the smooth specimen (lack of notches) in Figure 10 (blunt U notch) shows that the lifetime of these specimens is longer (more cycles) than the specimens with notches and with lower energy quantities. This implies that a high concentration of energy is present in specimens with notches.

Figure 11 shows approximations of the mean local energy SED by power equations of the experimental values for the different notches. Table 2 gives the approximation equations of all the notches with correlations coefficients. For a sharp V-notch, the critical volume becomes a circular sector of radius Rc centered at the notch tip (Fig. 6). For a blunt notch under mixed-mode loading, the critical volume is no longer centered at the notch tip, but rather at the point where the principal stress reaches its maximum value along the border of the notch (Fig. 7).

It was fundamentally assumed that the crescent-shaped volume rotates rigidly under mixed mode, with no change in shape and size (Fig. 7) [3]. The results obtained are in good agreement with the experimental results (Fig. 10).

Figure 12 shows the area where the first maximum principal stress (σ_{Imax}) is located for both U and V notches. For the V notch, the stress is located at the notch tip (Fig. 12a), whereas for the U notch the stress is located far from the notch tip, at the point where the notch lip begins (Fig. 12b).

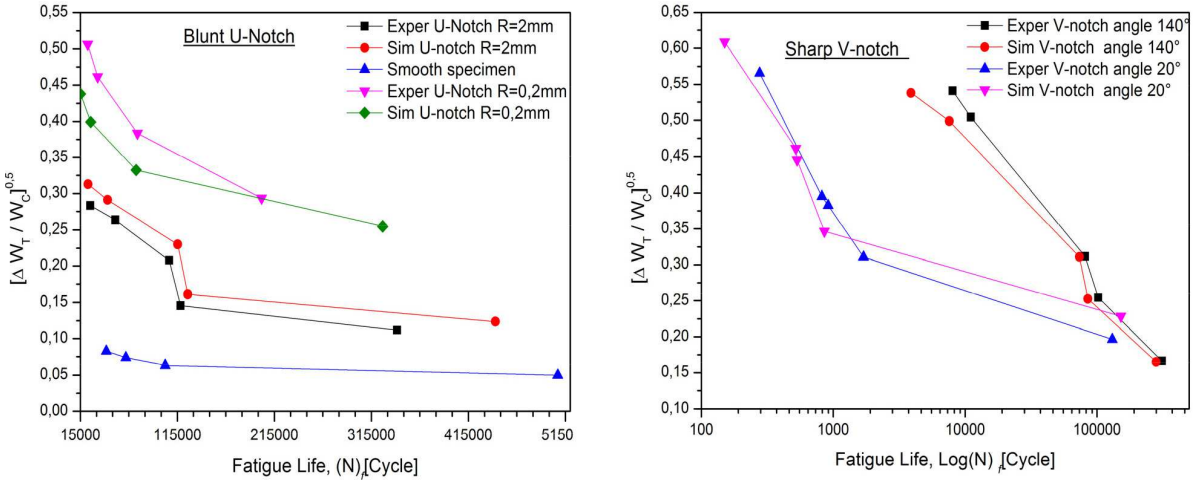


Fig. 10. Comparisons of experimental and simulation values of ASED for sharp V notch and blunt U notch via fatigue life

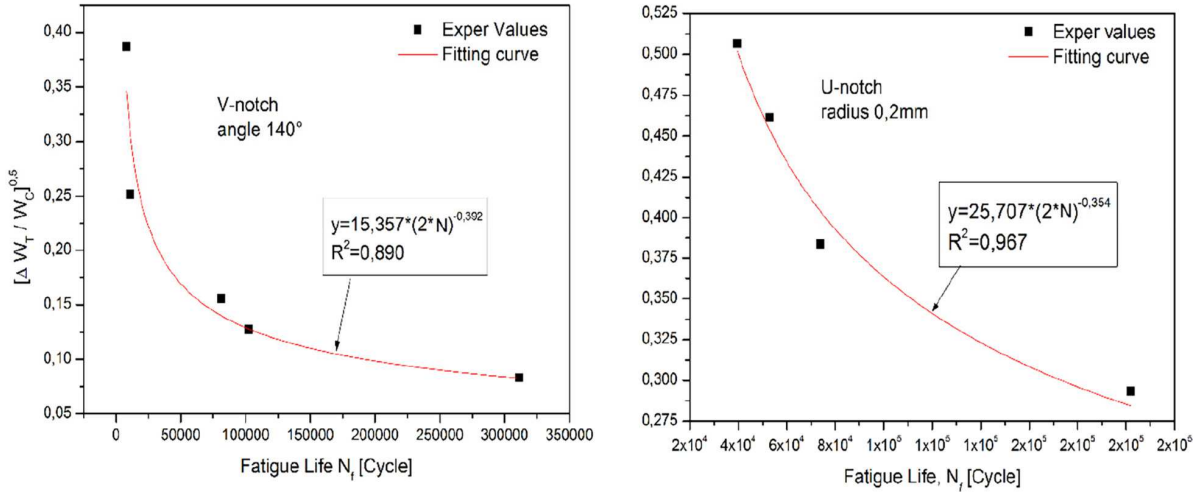


Fig. 11. Approximation of ASED via fatigue life

4.3. Loading effects on the local energy distribution of notched specimens

Another interest in this study is to analyze the variation of cyclic loading on the evolution of the average strain density energy under the effect of the presence of notches. Figures 13 and 14 show the distribution of the average strain energy normalized by critical energy via fatigue life: the high loads develop high- amplitude average SEDs. For low angles in V notches, the intensity of the average SED is greater than for more open angles. The lifetime is reduced compared to the more open angles. The values obtained by numerical calculation are in good approximation compared with those of the experimental ones.

For U-shaped notches with a significant radius, the high loading leads to high mean SED values compared to low-radius notches and a longer lifetime compared to sharp notches. Sharp V-notches develop higher mean SED values than blunt notches. This suggests that the loading amplitude plays an influential role on the ASED and the fatigue life of structures subjected to bending fatigue.

Table 2. Local energy modeling near notch

Experimental		
Notch type	**Correlation coefficients**	**Experimental: Local energy near notch**
U-notch radius 0.2 mm	$R^2 = 0.9881$	$W_{U0.2} = 6,1122.(2N)^{-0.248}$
V-notch angle 20°	$R^2 = 0.9591$	$W_{V20} = 0,9019.(2N)^{-0.13}$
V-notch angle 140°	$R^2 = 0.9656$	$W_{U140} = 10,939.(2N)^{-0.325}$
U-notch radius 2 mm	$R^2 = 0.8875$	$W_{U2} = 14,731.(2N)^{-0.381}$
Simulation		
Notch type	**Correlations coefficients**	**Simulation: Local energy near notch**
U-notch radius 0.2 mm	$R^2 = 0.967$	$W_{U0.2} = 25.707.(2N)^{-0.354}$
V-notch angle 20°	$R^2 = 0.857$	$W_{V20} = 1.944.(2N)^{-0.2093}$
V-notch angle 140°	$R^2 = 0.890$	$W_{U140} = 15.357.(2N)^{-0.392}$
U-notch radius 2 mm	$R^2 = 0.8305$	$W_{U2} = 12.483.(2N)^{-0.37}$

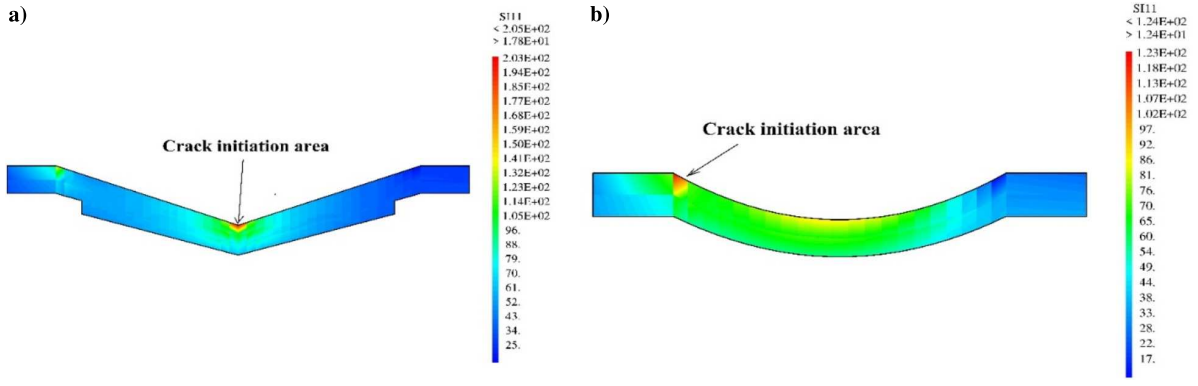


Fig. 12. Location of the zone of maximum principal stress (crack initiation zone) for (a) U notch R = 2 mm and (b) V notch $2\alpha = 140°$

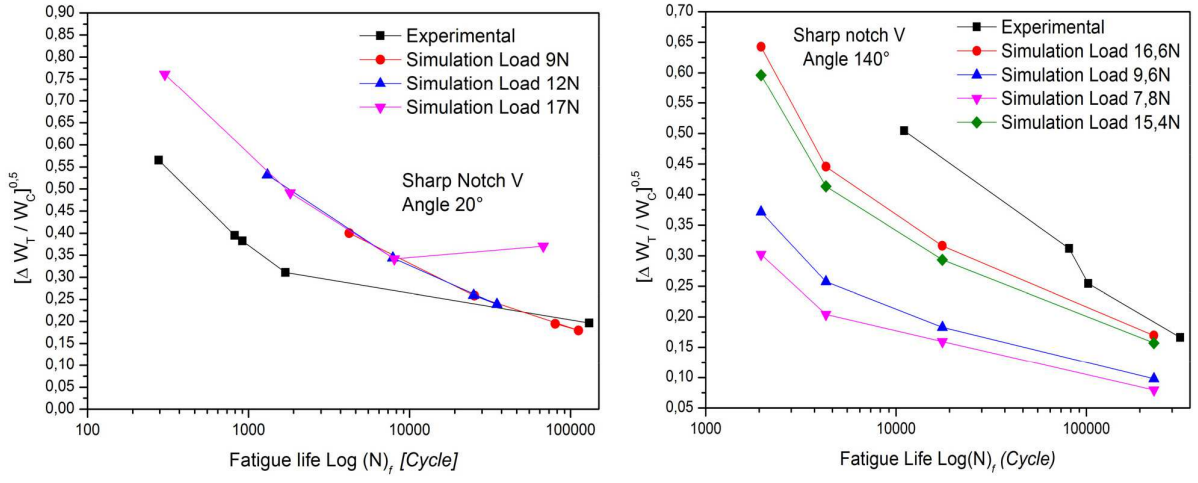


Fig. 13. Effect of loading on averaged energy density for V-notch via fatigue life (logarithmic values)

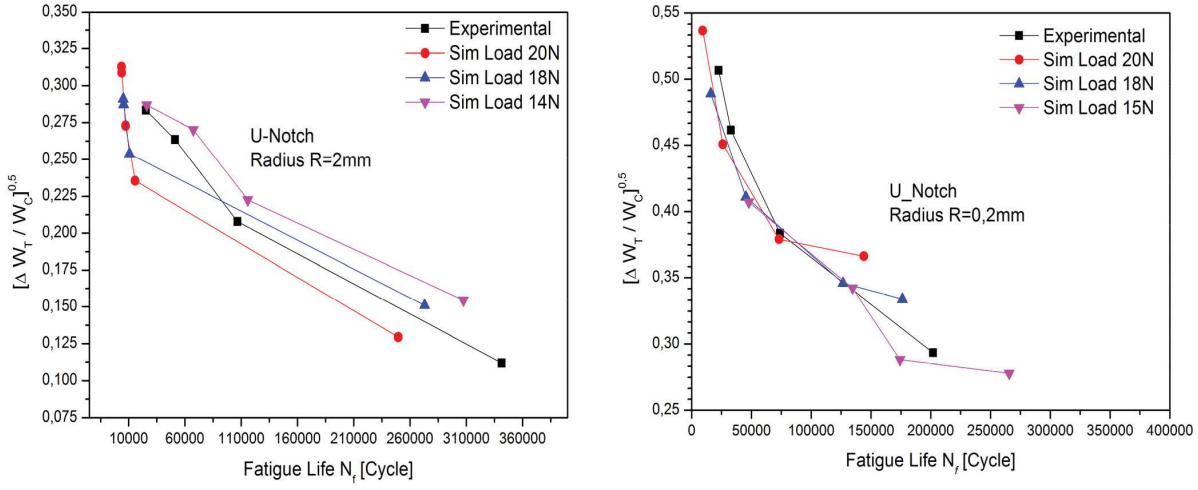


Fig. 14. Effect of loading on averaged energy density blunt U notch

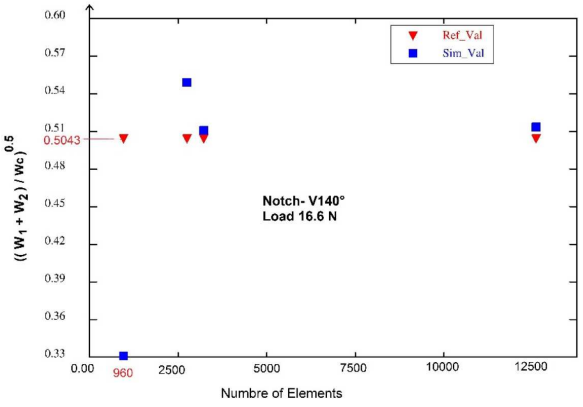


Fig. 15. Effect of the number of mesh elements

4.4. Effect of mesh on the results

Several simulations were performed for a sharp notch V140° at different mesh element numbers. Figure 15 shows convergence to the reference result from a mesh element number of 3224 elements. As the mesh element number increases, the results tend to deviate from the reference value.

4.5. Summary statistics of experimental and simulation tests

A statistical calculation was performed to compare the experimental and numerical results. The results of the calculation showed a good correlation between the two sets of results. The standard deviation of the experimental test results was slightly lower than that of the simulation test results. The minimum and maximum values of the two data sets were also very close (see Table 3).

5. Conclusions

The combination of two numerical tools, the extended finite element method (XFEM) and the local strain energy density approach, allowed us to analyze the influence of the presence of notches on the fatigue behavior of structures subjected to rotating bending.

The mixed loading mode appropriate for this type of solicitation allowed us to consider the combination of two modes, I and II. Under these conditions, we used two methods: experimental and numerical. The projection of the experimental work onto the numerical led to the ability to project the degree of fatigue of rotary bending into a two-dimensional bending specimen.

The study carried out identified the following results:

- A high concentration of local energy is around the notch tip,
- The value of the average strain energy density acting on the control volume zone differs from one notch to another. For the sharp notch the control volume is located in a circular area in the center, which is located at

Table 3. Correlations of experimental and numerical results

Experimental test							
Notch type	**Number of test repetitions**	**Min. number of cycles**	**Max. number of cycles**	**Standard deviation of cycles**	**Minimum energy**	**Maximum energy**	**Standard deviation of energy**
U-notch radius 0.2 mm	4	22640	201,865	82391.597	0.293	0.507	0.094
V-notch angle 20°	4	521,218	151,883	75622.87	0.229	0.461	0.107
V-notch angle 140°	4	11032	311,170	129198.70	0.166	0.504	0.143
U-notch radius 2 mm	5	25,239	341,478	125086.76	0.112	0.283	0.074
Simulation tests							
Notch type	**Number of test repetitions**	**Min number of cycles**	**Max number of cycles**	**Standard deviation of cycles**	**Minimum of energy**	**Maximum of energy**	**Standard deviation of energy**
U-notch radius 0.2 mm	4	15254	326,645	146,519.222	0.255	0.438	0.080
V-notch angle 20°	5	150.43	151,883	67,693.93	0.229	0.609	0.141
V-notch angle 140°	4	3890.97	85,337	42857.97	0.253	0.538	0.139
U-notch radius 2 mm	5	22938.2	442,920	169,677.83	0.124	0.313	0.081

the notch tip and the maximum of the principal stress is at the notch tip where the crack initiation zone is. In the case of blunt notches, the control volume is assumed to have a crescent shape, its maximum width is measured along the bisector of the notch,

– In mixed-mode case, the maximum principal stress occurs at a point on the edge of the notch, outside the bisector. The control volume is no longer centered on the bisector of the notch but turned rigidly with respect to it and located far from the point of the notch tip at the beginning of the notch lip end.

In components weakened by a notch subjected to rotational bending fatigue, the control volume follows the crack tip as it propagates, so that the fracture process zone begins and mode I remains the dominant mode. The local energy magnitude for a blunt notch is lower than that for a sharp notch, and the lifetime is longer for blunt notches. Therefore, the lifetime of components is affected by the presence of notches. The current work showed good concordance between experimental results and numerical results.

References

[1] Torabi A, Campagnolo A, Berto F. Local strain energy density to predict mode II brittle fracture in Brazilian disk specimens weakened by V-notches with end holes. *Mater Des.* 2015;69: 22–9.

[2] Moussaoui M, et al. Brittle fracture investigation from disc specimen weakened by U-notch in mixed mode I+ II. *Eng Solid Mech.* 2020;8(4): 337–52.

[3] Torabi A, Berto F. Strain energy density to assess mode II fracture in U-notched disk-type graphite plates. *Int J Damage Mech.* 2014;23(7): 917–30.

[4] Berto F, Lazzarin P. Fatigue strength of Al7075 notched plates based on the local SED averaged over a control volume. *Sci China Phys. Mech Astron.* 2014;57(1): 30–38.

[5] Berto F, Campagnolo A, Welo T. Local strain energy density to assess the multiaxial fatigue strength of titanium alloys. *Frat Integrità Strutt.* 2016;10(37): 69–79.

[6] Braun M, et al. Extension of the strain energy density method for fatigue assessment of welded joints to sub-zero temperatures. *Fatigue Fract Eng Mater Struct.* 2020;43(12): 2867–82.

[7] Berto F, Razavi S, Torgersen J. Frontiers of fracture and fatigue: Some recent applications of the local strain energy density. *Frat Integrità Strutt.* 2018;12(43): 1–32.

[8] Lazzarin P, Zambardi R. A finite-volume-energy based approach to predict the static and fatigue behavior of components with sharp V-shaped notches. *Int J Fract.* 2001;112(3): 275–98.

[9] Berto F, Lazzarin P. The volume-based Strain Energy Density approach applied to static and fatigue strength

assessments of notched and welded structures. *Proc Eng.* 2009;1(1): 155–8.

[10] Aliha M, et al. Mixed mode I/II fracture investigation of Perspex based on the averaged strain energy density criterion. *Phys Mesomech.* 2017;20(2): 149–56.

[11] Aliha M, et al. On the applicability of ASED criterion for predicting mixed mode I + II fracture toughness results of a rock material. *Theor Appl Fract Mech.* 2017;92: 198–204.

[12] Negru R, et al. Assessment of brittle fracture for PUR materials using local strain energy density and theory of critical distances. *Theor Appl Fract Mech.* 2015;79: 62–9.

[13] Ayatollahi M, Berto F, Lazzarin P. Mixed mode brittle fracture of sharp and blunt V-notches in polycrystalline graphite. *Carbon.* 2011;49(7): 2465–74.

[14] Berto F, et al. Local strain energy density to predict size-dependent brittle fracture of cracked specimens under mixed mode loading. *Theor Appl Fract Mech.* 2016;86: 217–24.

[15] Salavati H., et al. A new expression to evaluate the critical fracture load for bainitic functionally graded steels under mixed mode (I+II) loading. *Eng Fail Anal.* 2015;48: 121–36.

[16] Li Y, Fantuzzi N, Tornabene F. On mixed mode crack initiation and direction in shafts: strain energy density factor and maximum tangential stress criteria. *Eng Fract Mech.* 2013;109: 273–89.

[17] Sih GC Strain-energy-density factor applied to mixed mode crack problems. *Int J Fract.* 1974;10(3): 305–21.

[18] Sih GC. Mechanics of fracture initiation and propagation: surface and volume energy density applied as failure criterion. ©Springer Science+Business Media Dordrecht Originally published by Kluwer Academic Publishers in 1991.

[19] Sih G, Macdonald B. Fracture mechanics applied to engineering problems-strain energy density fracture criterion. *Eng Fract Mech.* 1974;6(2): 361–86.

[20] Sih G, Cha B. A fracture criterion for three-dimensional crack problems. *Eng Fract Mech.* 1974;6(4): 699–723.

[21] Berto F, Lazzarin P. A review of the volume-based strain energy density approach applied to V-notches and welded structures. *Theor Appl Fract Mech.* 2009;52(3); 183–94.

[22] Abolghasemzadeh M, Alizadeh Y, Mohammadi H. Fatigue strength reduction factors based on strain energy density applied to sharp and blunt notches under multiaxial loading. *Phy Mesomech.* 2020;23(1): 66–80.

[23] Williams M. Stress singularities resulting from various boundary conditions in angular corners of plates in extension. *Journal of Applied Mechanics* 1952;19(4): 526-28.

[24] Luo P, et al. Fatigue evaluation of rib-to-deck welded joint using averaged strain energy density method. *Eng Struct.* 2018;177: 682–94.

[25] Lazzarin P, Tovo R. A unified approach to the evaluation of linear elastic stress fields in the neighborhood of cracks and notches. *Int J Fract.* 1996;78(1): 3–19.

[26] Berto F, Razavi S, Ayatollahi M. Some methods for rapid evaluation of the mixed mode NSIFs. *Procedia Struct Integr.* 2017;3: 126–34.

[27] Berto F, Campagnolo A, Lazzarin P. Fatigue strength of severely notched specimens made of Ti–6Al–4V under multiaxial loading. *FF EMS.* 2015;38(5): 503–17.

[28] Berto F, Gallo P. Extension of linear elastic strain energy density approach to high temperature fatigue and a synthesis of Cu-Be alloy experimental tests. *Eng Solid Mech.* 2015;3(2): 111–6.

[29] Kim YW, et al. Energy-based approach to predict the fatigue life behavior of pre-strained Fe–18Mn TWIP steel. *Mater Sci Eng: A.* 2011;528(13–14): 4696–702.

[30] Mi C, et al. An energy-based method for lifetime assessment on high strength steel welded joints under different pre-strain levels. *Materials.* 2022;15(13): p4558 NPAG12p.

[31] You X, et al. Low cycle fatigue behaviour and life prediction of Q345B steel and its welded joint. *Mater Res Innov.* 2015;19(Sup 5): S5-1299–S5-1303.

[32] Gallo P, Berto F. Advanced materials for applications at high temperature: fatigue assessment by means of local strain energy density. *Adv Eng Mater.* 2016;18(12): 2010–7.

[33] El Haddad M, Topper T, Smith K. Prediction of nonpropagating cracks. *Eng Fract Mech.* 1979;11(3): 573–84.

[34] Lazzarin P, et al. Local strain energy density and fatigue strength of welded joints under uniaxial and multiaxial loading. *Eng Fract Mech.* 2008;75(7): 1875–89.

[35] Lazzarin P, Berto F. Some expressions for the strain energy in a finite volume surrounding the root of blunt V-notches. *Int J Fract.* 2005;135(1): 161–85.

[36] Meneghetti G, et al., Crack initiation life in notched Ti-6Al-4V titanium bars under uniaxial and multiaxial fatigue: synthesis based on the averaged strain energy density approach. *Frattura ed Integrità Strutturale*, 2017;11(41): Pages 8–15. doi: 10.3221/IGF-ESIS.41.02

[37] Berto F, et al. Fracture assessment of U-notches under mixed mode loading: two procedures based on the 'equivalent local mode I'concept. *Int J Fract.* 2007;148(4): 415–33.

[38] Gómez F, et al. Local strain energy to assess the static failure of U-notches in plates under mixed mode loading. *Int J Fract.* 2007;145(1): 29–45.

[39] Negru R, et al. Notch effect assessment in a PUR material using a ring shaped specimen. *Theor Appl Fract Mech.* 2018;97: 500–6.

[40] Lazzarin P, Zappalorto M, Berto F. Averaged strain energy density and J-integral for U-and blunt V-shaped notches under torsion. *Int J Fract.* 2014;188(2): 173–86.

Received 2023-05-12
Accepted 2023-10-02